Gluon Field Dynamics in Ultra-Relativistic Heavy-Ion Collisions: Time evolution on a Gauge Lattice in 3+1 Dimensions

W. Pöschl and B. Müller
Department of Physics, Duke University, Durham, NC 27708-0305, USA
(February 9, 2008)

We describe the dynamics of gluons and quarks in a relativistic nuclear collision, within the framework of classical mean-field transport theory, by the coupled equations for the classical Yang-Mills field and a collection of colored point particles. The particles represent the valence quarks in the colliding nuclei. We explore the time evolution of the gauge field in a numerical simulation of the collision of two Lorentz-boosted "nuclei" on a long three-dimensional gauge lattice. We report first results on soft gluon scattering and coherent gluon radiation.

Experiments with relativistic heavy ions at center-of-mass energies reaching 100 GeV/u will soon search for a new phase of nuclear matter, the quark-gluon plasma [1,2]. One of the theoretical challenges in this context is the development of a description on the basis of quantum chromodynamics (QCD) of the processes that may lead to the formation of locally equilibrated superdense matter in these nuclear reactions.

The possibility of a description of inelastic gluon processes by means of the nonlinear interactions of classical color fields has been proposed some time ago [3,4]. Recently, this scenario was examined in studies of the collision of two transverse polarized Yang-Mills field wave packets on a one-dimensional gauge lattice [5]. These calculations showed that the interaction between localized classical gauge fields can lead to the excitation of long wavelength modes in a way that is reminiscent of the formation of a dense gluon plasma.

Here we address the question to which extent soft gluon scattering in ultra-relativistic nuclear collisions contributes to the excitation of gluonic modes with non-vanishing transverse momentum and, therefore, to the conversion of longitudinal kinetic energy into transverse energy. The colliding gluon fields are generated by classical color sources, representing the fast moving nuclear valence quarks. The inclusion of particles also permits a comparison with perturbative calculations of gluon radiation from colliding quarks [6,7].

A set of equations describing the evolution of the phase space distribution of quarks and gluons in the presence of a mean color field, but in the absence of collisions, was proposed by Heinz [8,9]. This non-Abelian generalization of the Vlasov equation can be considered as the continuum version of the dynamics of an ensemble of classical point particles endowed with color charge and interacting with a mean color field. Denoting the space-time positions, momenta, and color charges of the particles by x_i^μ, p_i^μ and q_i^a, respectively, where $i = 1, \ldots, N$ is the particle index, the equations [10] for this dynamical system read:

$$m\frac{dx_i^\mu}{d\tau} = p_i^\mu \tag{0.1}$$

$$m\frac{dp_i^\mu}{d\tau} = g q_i^a F_a^{\mu\nu} p_{i,\nu} \tag{0.2}$$

$$m\frac{dq_i^a}{d\tau} = -g f^{abc} q_i^b p_i^\mu A_\mu^c. \tag{0.3}$$

Here g is the gauge coupling constant, f^{abc} are the structure constants of the gauge group (here taken as SU(2)), and $F_a^{\mu\nu}$ denotes the strength of the mean color field A_μ^c. The moving particles generate a color current $\mathcal{J}^\mu = J_a^\mu \tau^a/2$ which forms the source term of the inhomogeneous Yang-Mills equations

$$D_\mu \mathcal{F}^{\mu\nu}(x) \;=\; g\,\mathcal{J}^\nu(x) \;=\; g\sum_i \mathcal{Q}_i(t)\frac{p_i^\nu}{m}\delta(\vec{x}-\vec{x}_i(t)), \tag{0.4}$$

for the mean color field. These equations have recently been used in the weak-coupling limit ($g \ll 1$) to simulate the effects of hard thermal loops [12] on the dynamics of soft modes of a non-Abelian gauge field at finite temperature [13,14]. In this case, the colored particles describe the gauge field modes with thermal momenta, and the mean field describes the coherent motion of those gauge field modes which have a wave number k much smaller than the temperature T and are highly occupied.

Here we use Eq. (0.1–0.4) to describe the interactions among the soft glue field components of two colliding heavy nuclei. Transverse modes are included by using a 3-dimensional spatial lattice. The short-distance lattice cut-off a separates the regime in transverse momentum where the dynamics of gluons is perturbative (large k_T) from that where perturbation theory fails (small k_T) and which is of interest to us here. The interaction with the mean color field allows for an exchange of an arbitrary number of soft gluons. In combination with a parton cascade, the screening of the soft components of the gauge field by perturbative partons [15,16] is taken into account naturally by the nonlinear nature of the coupled Eq. (0.1–0.4). This will be discussed in a separate publication [17].

We represent the valence quarks of the two colliding nuclei as point particles moving in the space-time continuum, and interacting with a classical gauge field defined on a spatial lattice in continuous time. Here we neglect the collision integrals describing hard interactions between the particles. In the spirit of the statistical nature of the transport theory, we split each quark

into a number n_q of test particles, each of which carries the fraction $q_0 = Q_0/n_q$ of the quark color charge Q_0. For the gauge group SU(2) adopted here, each nucleon is represented by two quarks, initially carrying opposite color charge. A lattice version of the continuum equations (0.1–0.4) is constructed [13] by expressing the field amplitudes as elements of the corresponding Lie algebra, i.e. $\mathcal{A}_\mu, \mathcal{F}_{\mu\nu}, \mathcal{E}_k, \mathcal{B}_k \in \mathrm{LSU}(2)$. As in the Kogut-Susskind model of lattice gauge theory [18] we choose the temporal gauge $\mathcal{A}_0 = 0$ and define the following variables.

$$\mathcal{U}_{x,l} = \exp(-iga_l\mathcal{A}_l(x)) \;=\; \mathcal{U}^\dagger_{x+l,-l} \tag{0.5}$$

$$\mathcal{U}_{x,kl} = \mathcal{U}_{x,k}\,\mathcal{U}_{x+k,l}\,\mathcal{U}_{x+k+l,-k}\,\mathcal{U}_{x+l,-l} \tag{0.6}$$

Consequently, we have

$$\mathcal{E}_{x,j} = \frac{-i}{ga_j}\dot{\mathcal{U}}_{x,j}\mathcal{U}^\dagger_{x,j}\,, \quad \mathcal{B}_{x,j} = \frac{i\,\epsilon_{jkl}}{4ga_ka_l}\left(\mathcal{U}_{x,kl} - \mathcal{U}^\dagger_{x,kl}\right) \tag{0.7}$$

for the electric and magnetic fields, respectively. The lattice constant in the spatial direction j is denoted by a_j. As one can see from (0.5), the gauge field is expressed in terms of the link variables $\mathcal{U}_{x,l} \in \mathrm{SU}(2)$, which represent the parallel transport of a field amplitude from a site x to a neighboring site $(x+l)$ in the direction l. We choose $\mathcal{U}_{x,i}$ and $\mathcal{E}_{x,i}$ as the basic dynamic field variables and solve the following equations of motion

$$\dot{\mathcal{U}}_{x,k}(t) = i\,g\,a_k\,\mathcal{E}_{x,k}(t)\,\mathcal{U}_{x,k}(t) \tag{0.8}$$

$$\dot{\mathcal{E}}_{x,k}(t) = -\,\mathcal{J}_{x,k}(t) \;+\; \frac{i}{2ga_1a_2a_3}\sum_{l=1}^{3}\Big\{\mathcal{U}_{x,kl}(t) - \mathcal{U}^\dagger_{x,kl}(t) \tag{0.9}$$
$$-\,\mathcal{U}^\dagger_{x-l,l}(t)\left(\mathcal{U}_{x-l,kl}(t) - \mathcal{U}^\dagger_{x-l,kl}(t)\right)\mathcal{U}_{x-l,l}(t)\Big\}.$$

Subsequently, we present results of a calculation which corresponds to a central collision of two Pb nuclei. We assume that 16 nucleons in a row collide on the collision axis (3-axis). In accordance with the spatial extension of a nucleon we choose a lattice extension of 1.2 fm into both transverse directions. The lattice spacing is taken $a_j = 0.3$ fm in each direction, thus $4^2 \times 40$ lattice points cover the volume of 8 nucleons in one row. The coverage of two complete nuclei requires much larger lattices and remains a challenge for more extended calculations in the future. The lattice is closed to a 3-torus and a dual lattice is superimposed on the original lattice in such a way that the lattice points are located in the centers of the cells of the dual lattice. The dual lattice cells are used to associate particles with lattice sites and thus to define the source terms in (0.4).

To generate the initial configurations of the nuclei we randomly distribute color charged massless particles over the volume such that each lattice cell is occupied by an even number n_b of particles. The total initial charge is zero in each box corresponding to a neutral charge distribution. Momenta with opposite but random directions and Boltzmann distributed absolute values are assigned to each pair of particles. The equilibrium configuration of a single nucleus in its rest frame is obtained through the evolution of (0.1–0.3, 0.8, 0.9) over a long period of time starting from the initial fields $\mathcal{E}_{x,k}(t=0) = 0$, $\mathcal{U}_{x,k}(t=0) = \mathbf{1}_2$. As shown in Table 1, we find ratios between field energy W_f and total energy W_tot which descend smoothly from $W_\mathrm{f}/W_\mathrm{tot} = 0.45$ to $W_\mathrm{f}/W_\mathrm{tot} = 0.14$ for particle densities $n_b = 2$ to $n_b = 10$. In Table 1 we also demonstrate that the ratio does not depend on a, g, and Q_0. The ratio is also independent of the time step (if $\Delta t \le a/10$). For the large final times $t_n \approx 10^4$, the value of $W_\mathrm{f}/W_\mathrm{tot}$ has saturated, except for very small couplings, such as $g = 0.3$, where the equilibrium is reached only after longer times.

The simulation of a collision requires a Lorentz boost of each nucleus into the center of velocity frame of both nuclei. In the example presented below, the kinetic energy is 100 GeV/u for which $\gamma = 106.5$. Both nuclei are mapped into their initial positions on a large Lorentz-contracted lattice right after the boost of particle coordinates x_i, p_i and field amplitudes. We have investigated two ways to perform the boost. In one method we thermalise the nuclei first and apply the Lorentz transformation afterwards. This method is complicated and requires a continuation of the time-evolution throughout the boost. Furthermore, the lattice dispersion relation is not Lorentz invariant and therefore it does not lead to a stable translation of the nuclei on the lattice after the boost.

More successful is a boost of the particle coordinates x_i, p_i at time $t = 0$ for both nuclei, wherafter the fields are generated from the initial conditions $\mathcal{E}_{x,k}(t=0) = 0$ and $\mathcal{U}_{x,k}(t=0) = \mathbf{1}_2$. This method leads to quasi-stable configurations propagating over distances which extend over several thousand lattice points in the longitudinal direction. However, it requires large initial distances between the nuclei because an equilibrium between particles and fields has to be established before the collision. For nucleons with the correct mass ($m_n = 939$ MeV) about 50% of the total energy are carried by glue fields. For the above chosen lattice constants each nucleon is covered by 80 lattice cells and thus, according to the results in Table 1, each quark must be split into $n_q = 160$ particles to obtain a ratio close to $W_\mathrm{f}/W_\mathrm{tot} = 0.5$ at equilibrium. In order to reproduce the correct nucleon mass the particle momenta have to be smaller by a factor $1/n_q$ on average in comparison to the momenta of the quarks. The field energy associated with a single link can then occasionally exceed the kinetic energy of a particle resulting in the emission of particles due to backwards scattering from the link. This corresponds to the (unphysical) emission of nucleons from the moving nuclei, which we want to avoid.

As long as we are only interested in the dynamics of the glue fields we may increase the momenta of the particles such that the particle distributions of the nuclei remain stable throughout the whole collision. Therefore, in order to prepare a stable initial state for the collision, we start (before the Lorentz boost) with an initial condi-

tion in which the momenta of the particles are generated at a fictitious temperature of $T_p = 100$ GeV. The directions of the momenta are randomly distributed into the forward hemisphere such that pairs of particles have opposite transverse momenta. We found that the final results are quite independent of the initial condition. These initial conditions, however, contain much higher total energy $W'_{\rm tot}$ than $W_{\rm tot}$ and are unphysical. The fact that the temperature of the gluon field $T \ll T_p$ is limited by $T_{max} = 1.3$ GeV due to the lattice cutoff prevents the field energies from becoming too large. Furthermore, we increase the value for n_b to keep the ratio $W_{\rm f}/W_{\rm tot}$ small while $W_{\rm tot} \ll W'_{\rm tot}$. For $n_b = 6$ choosen, an initial separation d_0 of more than 12000 lattice spacings is necessary to approach a ratio of about $W_f/W_{\rm tot} = 0.5$. d_0 is Lorentz contracted to 33.8 fm in the center of velocity frame. According to the above fixed extensions into transverse directions and size of the nuclei we use a lattice that comprises a total of $4^2 \times 12100$ points. While the nuclei translate on the lattice, we adiabatically increase the coupling constant with a rate of $\Delta g/\Delta t \leq (5000a)^{-1}$. After g has reached its final value ($g = 2.0$), we continue the time evolution until $W_{\rm f}/W_{\rm tot} \approx 0.5$.

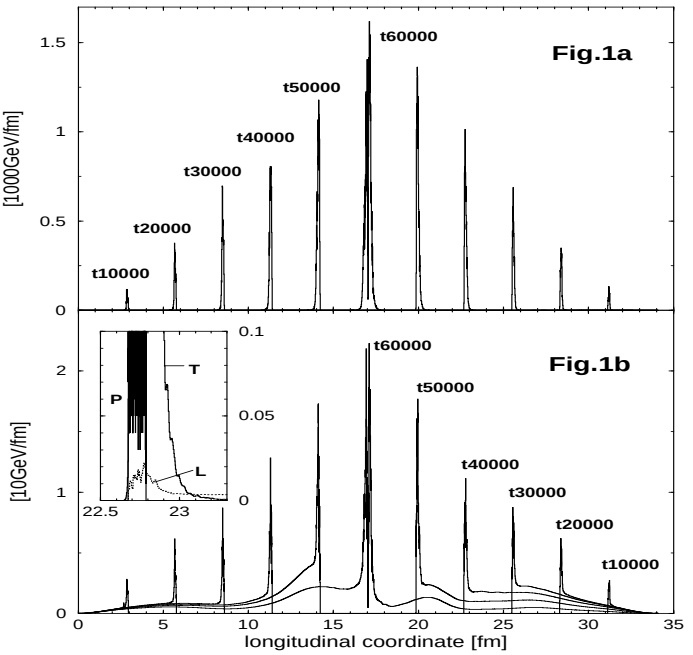

FIG. 1. Transverse and longitudinal E-field energy densities at various times before the collision.

In the following, we call the direction $j = 3$ which is parallel to the collision axis the "longitudinal" direction and E-field amplitudes associated with longitudinal links are called the "longitudinal fields" $E_{\rm l}$. The fields $E_{\rm t}$ in transverse directions are called "transverse". Figures 1a,b display the field energy densities $w_{\rm t}^{(E)}(z) = Tr(\mathcal{E}_1\mathcal{E}_1) + Tr(\mathcal{E}_2\mathcal{E}_2)$, (see Fig. 1a) and $w_{\rm l}^{(E)}(z) = Tr(\mathcal{E}_3\mathcal{E}_3)$ (see Fig. 1b) for both, transverse and longitudinal compontents of the E-field every 10000 time steps. A time-step width of 0.03 fm has been used. We verified, that the corresponding B-field energy densities $w^{(B)}(z)$ are identical with $w_{\rm t}^{(E)}(z)$. After 1000 time steps (not shown in the figure) the transverse E-field energy $W_{\rm t}^{(E)}$ is by about a factor $\gamma/2$ larger than the longitudinal E-field energy $W_{\rm l}^{(E)}$. This ratio increases to γ at 50000 time steps and remains constant afterwards.

As Fig. 1a shows, two configurations representing two nuclei propagate remarkably stably (nucleus 1 from left to right and nucleus 2 from right to left) over long distances on the lattice. In the upper left corner of Fig. 1b at time step 40000, the particle density (P), which is defined as the number of particles per bin of width $a/10$ in longitudinal direction, is superimposed on the transverse (T) and longitudinal (L) field energy densities for comparison. The particle density defines the extension of the nucleus in the longitudinal direction. The mismatch between particle density and field energy density decreases when the density of lattice points covering the nucleus in the longitudinal direction is increased. This requires a shift of the cutoff (here at $k_c = 2.0$ GeV for $a = 0.3$ fm) to higher momenta.

The tails of the field energy densities result not only from lattice dispersion effects. The lattice is Lorentz contracted in the longitudinal direction and particles have large longitudinal momentum components. Therefore, particles primarily transfer energy into longitudinal links. The nonlinearity of the Yang Mills equations provides a mechanism transferring energy from longitudinal into transverse degrees of freedom. Field amplitudes which are left behind on the longitudinal links are cancelled by following particles of rotated color charge. Fig. 1b shows that this cancellation does not work perfectly, and small, but long tails remain behind the nuclei. The amplitude of these tails decreases for increasing n_b and d_0. Another advantage of choosing n_b large is to avoid artificial excitation of high frequency modes caused by an interplay of lattice discretization and point-like charges.

Fig. 2a and Fig. 2b display $w_{\rm t}^{(E)}(z)$ and $w_{\rm l}^{(E)}(z)$ at 4000, 8000, 12000 and 16000 time steps after the collision. The particle densities are superimposed to indicate the position and original extension of the nuclei. As compared to Fig. 1b (upper left window) the width of the distributions $w_{\rm t}^{(E)}(z)$ moving with the particles is considerably increased. At the begining of the collision we observe a kink in $W_{\rm f}(t)$, which increases remarkably in the collision. As we see from Fig. 2a, a considerable fraction of the transverse field energy is deposited around the center of collision between the receding nuclei. At time step 76000, about 30.1 GeV of the total transverse electric field energy $W_{\rm t}^{(E)} = 490.7$ GeV (at time step 60000) are left in the spatial region between 13.9 fm and 19.9 fm. Consequently, the energy density in the overlap region with the particles is reduced allowing an enhanced transfer of energy from the particles into the fields. This results in the kink in $W_{\rm f}(t)$.

Fig. 2b displays the corresponding longitudinal energy densities. The calculation shows that within short times ($\Delta t = 0.5\,\mathrm{fm}$) after the collision about 26 % (7.25 GeV) of the total field energy (28.03 GeV) left in the region between 16.4 fm and 17.4 fm are carried by longitudinal components of the E-field. The ratio $w_{\mathrm{l}}^{(E)}/w_{\mathrm{t}}^{(E)}$ in this region is 0.7 which is large compared to the above mentioned factor $1/\gamma$. Since the color charge and color current density is zero, the linearized equations (0.4) are homogeneous in this region and allow only for solutions with non-zero amplitudes into transverse directions in relation to the direction of their energy flow. Figure 2b displays the fraction with momenta pointing into transverse direction relative to the collison axis. A calculation with the right-hand side of (0.2) set to zero yields practically the same results, which finds its explanation in a transfer of energy from the propagating transverse fields to the longitudinal fields due to the non-linear coupling between E_{t} and E_{l} in (0.4). When the two nuclei overlap during the collision, the fields are superposed. As a result of the nonlinear terms in (0.4), which act as source terms for the longitudinal fields, the amplitudes E_{l} start to grow rapidly. This mechanism describes the scattering of soft gluons.

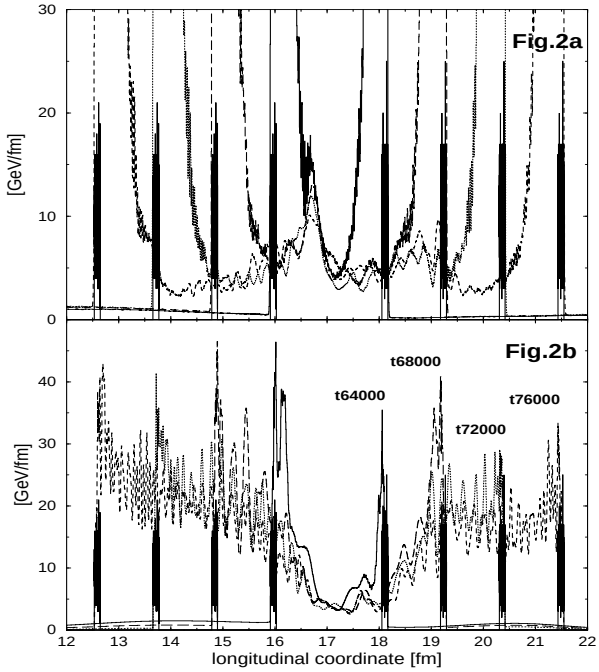

FIG. 2. Transverse and longitudinal E-field energy densities after the collision.

The distribution $w_{\mathrm{l}}^{(E)}(z)$ increases sharply for collision times larger 1.0 fm. When the two nuclei pass through each other, the particles experience the combined fields of both nuclei. The corresponding changes of the field amplitudes enter into the r.h.s. of (0.3) and modify the orientation of the color charge vectors $\vec{q}_i^{\,a}(t)$ during the rather short overlap time of 0.11 fm. This induces net color charge currents resulting in radiation of gluons. Since the longitudinal momenta of the particles are large compared with their transverse components, color charges move essentially parallel to longitudinal links and induce electric fields on these links. Before the collision, the charge of the following particles was polarized such that these fields were cancelled. After the collison this is no longer true. A continuation of the time evolution has shown that the longituinal energy density of the fields remains as large as in Fig. 2b and decreases slowly after time step 100000 (28.17 fm). These longitudinal fields possess only transverse momenta and result in gluon radiation into transverse directions.

The energy distribution in Fig. 2a and in particular the hump at the center of collision result from non-linear properties of Eq. (0.4) and exhibit the gluon-gluon interaction. We repeated the calculation for smaller initial distances d_0. It turned out that there is a threshold between $7000a$ and $9000a$ below of which the hump doesn't appear and $w_{\mathrm{t}}^{(E)}(z) < w_{\mathrm{l}}^{(E)}(z)$ between the receding nuclei. Further, $w_{\mathrm{t}}^{(E)}(z)$ is almost constant as a function of z in this case. As can be seen from Fig. 2a and 2b, above this threshold, we find $w_{\mathrm{t}}^{(E)}(z) > w_{\mathrm{l}}^{(E)}(z)$ in a small region around the center of collision. The slow decay of the hump indicates that essentially low frequent modes are excited in the collision of the fields. The transverse fields have momenta into longitudinal directions and thus describe longitudinal gluon radiation. A comparison of the transverse field energy deposit with the longitudinal field energy deposit for large times ($t/a = 76000$) shows that the radiation of soft gluons into longitudinal directions amounts to about 30% of the intensity into transverse directions.

The authors are thank S.A. Bass and S.G. Matinyan for discussions. This work was supported by the U.S. Department of Energy under Grant No. DE-FG02-96ER40495.

[1] J. W. Harris and B. Müller, *Annu. Rev. Nucl. Part. Sci.* **46**, 71 (1996)
[2] A.V. Smilga, *Phys. Rep.* **291**, 1 (1997).
[3] H. Ehtamo, J. Lindfors, and L. McLerran, *Z. Phys.* **C18**, 341 (1983).
[4] A. Kovner, L. McLerran, and H. Weigert, *Phys. Rev. D* **52**, 3809 and 6231 (1995).
[5] C.R. Hu, S.G. Matinyan, B. Müller, and A. Trayanov, *Phys. Rev. D* **52**, 2402 (1995).
[6] Yu.V. Kovchegov and D.H. Rischke, *Phys. Rev. C* **56**, 1084 (1997).
[7] S.G. Matinyan, B. Müller and D. Rischke, *Phys. Rev. C* **57** 1927 (1998).
[8] U. Heinz, *Phys. Rev. Lett.* **51**, 351 (1983); *Ann. Phys. (NY)* **161**, 48 (1985); **168**, 148 (1986)
[9] H.-Th. Elze and U. Heinz, *Phys. Rep.* **183**, 81 (1989)

[10] S.K. Wong, Nuovo Cim. **A 65**, 689 (1979)
[11] U. Heinz, Phys. Lett. **B 144**, 228 (1984)
[12] R. Pisarski, *Phys. Rev. Lett.* **63**, 1129 (1989); E. Braaten and R. Pisarski, *Phys. Rev. D* **42**, 2156 (1990).
[13] C.R. Hu and B. Müller, *Phys. Lett.* **B409**, 377 (1997)
[14] G.D. Moore, C.R. Hu and B. Müller, *Phys. Rev. D* **58**, 045001 (1998)
[15] T.S. Biró, B. Müller, and X.N. Wang, *Phys. Lett.* **B283**, 171 (1992)
[16] K.J. Eskola, B. Müller, and X.N. Wang, *Phys. Lett.* **B374**, 20 (1996)
[17] S.A. Bass, B. Müller, and W. Pöschl, Duke University preprint DUKE-TH-98-168 (nucl-th/9808011).
[18] J. Kogut and L. Susskind, *Phys. Rev. D* **11**, 395 (1975)

a [fm]	g	Q_0	n_b	t_n [a/10]	$W_{\rm f}/W_{\rm tot}$
1.0	1.0	2.0	2	$1 \cdot 10^4$	0.45
1.0	1.0	2.0	4	$1 \cdot 10^4$	0.30
1.0	1.0	2.0	6	$1 \cdot 10^4$	0.26
1.0	1.0	2.0	10	$1 \cdot 10^4$	0.14
0.1	1.0	2.0	2	$1 \cdot 10^4$	0.45
0.1	1.0	2.0	4	$1 \cdot 10^4$	0.30
0.3	1.0	2.0	2	$1 \cdot 10^4$	0.45
0.3	2.0	2.0	2	$1 \cdot 10^4$	0.46
0.3	3.0	2.0	2	$1 \cdot 10^4$	0.46
0.3	0.5	2.0	2	$1 \cdot 10^4$	0.37
0.3	0.5	2.0	2	$2 \cdot 10^4$	0.44
0.3	0.3	2.0	2	$1 \cdot 10^4$	0.19
0.3	0.3	2.0	2	$3 \cdot 10^4$	0.36
0.3	0.3	2.0	2	$6 \cdot 10^4$	0.45
0.3	2.0	1.0	2	$1 \cdot 10^4$	0.46
0.3	2.0	0.5	2	$1 \cdot 10^4$	0.46
0.3	2.0	0.3	2	$1 \cdot 10^4$	0.46

TABLE I. The ratio $W_{\rm f}/W_{\rm tot}$ is listed in dependence on the parameters a, g, Q_0, n_b for large times t_n when the configuration has evolved close to equilibrium.